Retraction: Dose dependency of *Disp1* and genetic interaction between *Disp1* and other hedgehog signaling components in the mouse

Hua Tian, Toyoaki Tenzen and Andrew P. McMahon *Development* **131**, 4021-4033.

A re-examination within our laboratory of two papers published by our group in *Development* (Tian et al., 2004; Tian et al., 2005) has revealed a duplication of Dr Tian's data in these papers. On review, we have found that the documentation underpinning a number of conclusions in Tian et al., 2004 is inadequate. As a consequence, we regret that we must retract Tian et al., 2004.

The principal conclusions in Tian et al., 2005 are supported by appropriate documentation. Nevertheless, to confirm the conclusions drawn from Dr Tian's primary data on the tissue requirement for Dispatched in facial development, we will repeat the experiments documented in Figure 2 of Tian et al., 2005, and will report our findings to the journal once these experiments have been concluded. We do not expect this re-analysis to change the conclusions drawn in this paper.

We apologize to the editors and readership of *Development*.

Andrew McMahon, Hua Tian* and Toyo Tenzen
Department of Molecular and Cellular Biology, Harvard University, 16 Divinity Avenue, Cambridge, MA 02138, USA
*Present address: 2548 Post Street, San Francisco, CA 94115, USA

References

Tian, H., Tenzen, T. and McMahon, A. P. (2004). Dose dependency of *Disp1* and genetic interaction between *Disp1* and other hedgehog signaling components in the mouse. *Development* **131**, 4021-4033.

Tian, H., Jeong, J., Harfe, B. D., Tabin, C. J. and McMahon, A. P. (2005). Mouse Disp1 is required in sonic hedgehog-expressing cells for paracrine activity of the cholesterol-modified ligand. *Development* **132**, 133-142.

Dose dependency of *Disp1* and genetic interaction between *Disp1* and other hedgehog signaling components in the mouse

Hua Tian, Toyoaki Tenzen and Andrew P. McMahon*

Department of Molecular and Cellular Biology, The Biolabs, Harvard University, 16 Divinity Avenue, Cambridge, MA 02138, USA
*Author for correspondence (e-mail: amcmahon@mcb.harvard.edu)

Accepted 7 May 2004

Development 131, 4021-4033
Published by The Company of Biologists 2004
doi:10.1242/dev.01257

Summary

Genetic analyses in *Drosophila* have demonstrated that a transmembrane protein Dispatched (Disp) is required for the release of lipid-modified Hedgehog (Hh) protein from Hh secreting cells. Analysis of *Disp1* null mutant embryos has demonstrated that *Disp1* plays a key role in hedgehog signaling in the early mouse embryo. Here we have used a hypomorphic allele in *Disp1(Disp1$^{\Delta 2}$)*, to extend our knowledge of Disp1 function in Hh-mediated patterning of the mammalian embryo. Through genetic combinations with null alleles of patched 1 (*Ptch1*), sonic hedgehog (*Shh*) and Indian hedgehog (*Ihh*), we demonstrate that Disp1 genetically interacts with Hh signaling components. As *Disp1* activity is decreased we see a progressive increase in the severity of hedgehog-dependent phenotypes, which is further enhanced by reducing hedgehog ligand levels. Analysis of neural tube patterning demonstrates a progressive loss of ventral cell identities that most likely reflects decreased Shh signaling as Disp1 levels are attenuated. Conversely, increasing available Shh ligand by decreasing *Ptch1* dosage leads to the restoration of ventral cell types in *Disp1$^{\Delta 2/\Delta 2}$* mutants. Together, these studies suggest that Disp1 actively regulates the levels of hedgehog ligand that are available to the hedgehog target field. Further, they provide additional support for the dose-dependent action of Shh signaling in patterning the embryo. Finally, in-vitro studies on *Disp1* null mutant fibroblasts indicate that Disp1 is not essential for membrane targeting or release of lipid-modified Shh ligand.

Supplemental data available online

Key words: Dispatched, Sonic hedgehog, Patched, Hypomorph, Mouse, Morphogenesis

Introduction

Development of multicellular organisms requires cell–cell interactions mediated by secreted signals. Among the most extensively characterized are members of the *hedgehog* (*Hh*) family, which regulate many processes during embryogenesis, including cell fate specification, cell proliferation and cell survival (reviewed by Ingham and McMahon, 2001). Mammals have three *Hh* genes: sonic hedgehog (*Shh*), Indian hedgehog (*Ihh*) and desert hedgehog (*Dhh*). Their diverse roles in the vertebrate embryo have been extensively reviewed (McMahon et al., 2003). *Shh* is essential for early patterning of the ventral central nervous system (CNS), somite, and anterior–posterior organization of the limb. Later in development, *Shh* is involved in the growth and morphogenesis of hair, tooth, lung, gut and kidney etc. *Ihh* coordinates growth and differentiation in the endochondral skeleton, while *Dhh* is required for development of peripheral nerve, testicular organization and spermatogenesis.

Given the importance of these genes in regulating many aspects of embryonic development, it is not surprising that aberrant Hh signaling activity underlies a number of human abnormalities and diseases. Those include notably holoprosencephaly (HPE) (Belloni et al., 1996; Nanni et al., 1999), a midline patterning defect characterized by incomplete separation of ventral forebrain into distinct cerebral hemispheres, polydactyly (Masuya et al., 1995), brachydactyly type A-1 (Gao et al., 2001), nerve sheath degeneration (Johnson et al., 1996) and a variety of cancers (McGarvey et al., 1998).

All Hh proteins are synthesized as full-length precursors that undergo autocatalytic cleavage to generate an N-terminal signaling fragment Hh-Np (‘p’ stands for processed) (reviewed by Ingham and McMahon, 2001). The mature Hh-Np ligand is dually lipid-modified with a C-terminal cholesterol and an N-terminal palmitate (Pepinsky et al., 1998; Porter et al., 1996). Both lipids are essential for tight membrane association and for full signaling strength of Hh molecules as demonstrated by in-vivo and in-vitro experiments (Chamoun et al., 2001; Taylor et al., 2001).

Despite the tight membrane association of the Hh ligand, an Hh signaling response can occur at considerable distances, as much as 150 to 200 μm in the vertebrate limb bud (Lewis et al., 2001). The first insights into how a membrane-associated Hh ligand travels from Hh-producing cells to its target field began to emerge with the identification of *dispatched* (*disp*) in *Drosophila* (Burke et al., 1999). Loss of Disp function results in a mutant phenotype that is similar to the loss of Hh; however, in *disp* mutants, Hh protein accumulates in the Hh-secreting cell, and a weak activation of target genes is detected but only in a single row of cells immediately adjacent to the Hh-

secreting cell. Thus, the bulk of Hh-Np produced in the secreting cell does not traffic into the target field. Further, genetic studies suggest that Disp functions exclusively in the Hh pathway, and its activity is required only within the Hh-secreting cell, specifically for releasing cholesterol-modified Hh-Np. Signaling by Hh-N, which lacks a cholesterol linkage, does not require Disp activity (Burke et al., 1999).

Disp, like the Hh receptor Ptch, is a multipass transmembrane protein that shares a putative sterol-sensing domain (SSD). This phylogenetically conserved SSD domain has been identified in key regulatory genes in cholesterol homeostasis and lipoprotein signaling. Mutations in the SSD generally result in loss of protein activity at least in part by altering the normal localization of the protein in distinct membrane compartments (Zhang et al., 2001a). By analogy to the function of other SSD proteins in trafficking processes and studies of *disp* mutants in *Drosophila*, Disp may regulate Hh trafficking within the synthesizing cells (Burke et al., 1999; Gallet et al., 2003).

Recently, three groups have reported on two mammalian Disp homologs, Disp1/A and Disp2/B (Caspary et al., 2002; Kawakami et al., 2002; Ma et al., 2002); herein we adopt the nomenclature Disp1 and Disp2 to be most consistent with the convention for mammalian gene families. Of the two murine Disp homologs, *Disp1* is expressed weakly but broadly at early stages of embryonic development, overlapping with reported *Shh* and *Ihh* expression domains (Kawakami et al., 2002). Two laboratories independently generated mouse *Disp1* null alleles, where exon 8 ($Disp1^{\Delta 8}$), which encodes most of the transmembrane spanning regions and C-terminal domain of Disp1, was removed (Kawakami et al., 2002; Ma et al., 2002). Notably, homozygous $Disp1^{\Delta 8}$ mutants do not survive beyond embryonic day (E) 9.5 and exhibit gross morphological features that are nearly identical to smoothened mutant embryos – the model for complete loss of Hh signaling activity (Zhang et al., 2001b). A third mutant with a point mutation in the second of two cysteine-rich putative extracellular domains ($Disp1^{C829F}$), generated in an N-ethyl-N-nitrosourea (ENU) chemical mutagenesis screen, gives rise to a similar mutant phenotype (Caspary et al., 2002). Thus, $Disp1^{C829F}$ does not appear to produce functional Disp1 protein and is most likely a null allele. Interestingly, in *Disp1* mutants, an Hh signaling response is retained in midline cells of the notochord that both express Shh and respond to Shh signals (Ma et al., 2002). But the absence of signaling in target fields that lie adjacent to the Hh-expressing cells leads to a failure of L-R axis determination and defective patterning of the ventral neural tube and somite.

As a result of the early embryonic lethality exhibited by *Disp1* null mutants (between E8.5 and 9.5), the investigation of Disp1 function in Hh-dependent signaling events at later developmental stages, the focus of most studies to date, is compromised. Further, as Hh signaling involves the transduction of a graded signal through multiple concentration thresholds, examining the tissue response in the context of modulated Hh release may provide novel insights into Hh action. To this end, new alleles of *Disp1*, in particular hypomorphic alleles, may be important. Here, we have taken advantage of a hypomorphic allele, $Disp1^{\Delta 2}$. Our findings are consistent with a model in which Disp1 controls the levels of available Hh signal in the embryo. Complementary cell culture studies suggest that secretion and cell-surface accumulation of Shh are both Disp1-independent processes.

Materials and methods

Molecular cloning and sequence analysis

Two expressed sequence tag (EST) clones with strong homology to *Drosophila Disp* were used to screen a mouse P1 brain cDNA library. Positive clones were picked and sequenced. From these clones and the original EST, the composite full-length sequences for Disp1 and Disp2 were assembled. The intron/exon boundaries were confirmed by RT-PCR and mouse genomic sequence available through Celera database. Three transmembrane domain prediction programs (TopPred 2, TMHMM, HMMTOP) all predicted 12 transmembrane domains. AlignX program from Vector NTI suite was used to align the sequences.

Mice

$Disp1^{C829F/+}$ mice were kindly provided by Kathryn Anderson (Caspary et al., 2002). The $Ptch1^{null}$ and Shh^{null} alleles have been described previously (Goodrich et al., 1996; St-Jacques et al., 1998). Mutations were studied on mixed genetic background.

Generation of $Disp1^{\Delta 2/\Delta 2}$ mutant

To remove exon 2 of Disp1, a targeting vector was engineered in which exon 2 was flanked by loxP sites. After homologous recombination at the Disp1 locus in AV3 embryonic stem (ES) cells, a heterozygous ES cell line was injected into blastocysts of the C57BL6/J strain to generate chimeras. Chimeric males were bred with *β-actin-Cre* females to obtain $Disp1^{\Delta 2/+}$ heterozygous offspring.

RNA in-situ hybridization

Embryos were fixed in 4% paraformaldehyde at 4°C overnight. Whole-mount and section in-situ hybridization using digoxigenin-labeled RNA probes was performed as described previously (Schaeren-Wiemers and Gerfin-Moser, 1993; Wilkinson, 1992).

Immunohistochemistry

Rabbit polyclonal antibodies DspN and DspC were raised against bacterially expressed glutathione-S-transferase fusion proteins containing amino acids 1-100 and 1370-1521 of Disp1 respectively. The antiserums were affinity purified as described elsewhere (Bumcrot et al., 1995). For all antisera, inoculation of New Zealand White rabbits, as well as test and production bleeding, were carried out at Convance, Inc. Immunohistochemistry was performed as described for sections (Yamada et al., 1991) and whole mounts (Lewis et al., 2001). Antibody and dilutions were as follows: rabbit αShh, 1:100 (Marti et al., 1995); αHNF-3β, 1:8000 (Ruiz i Altaba et al., 1995); αNkx6.1, 1:3000 (Cai et al., 2000); αNkx2.2, 1:4000 (Briscoe et al., 1999); αOlig2, 1:5000 (Takebayashi et al., 2000); αChox10, 1:5000 (Briscoe et al., 2000), Mouse αNkx2.2 1:50 (Ericson et al., 1997a); αPax6,1:20 (Ericson et al., 1997b); αPax7, 1:20 (Ericson et al., 1996); αEn,1:30 (Developmental Studies Hybridoma Bank; DSHB); αEvx, 1:100 (Briscoe et al., 2000). αLim1/2, 1:100 (DSHB); αMNR2, 1:20 (DSHB).

Histology and skeletal preparations

For histological analysis, embryos were fixed in Bouin's fixative at 4°C overnight, then embedded in paraffin, sectioned at 8 μm, and stained with hematoxylin and eosin. For skeletal preparations, 18.5 days post coitum (dpc) embryos were processed as described previously (Karp et al., 2000).

Cell culture-based assay

$Disp1^{C829F/C829F}$ mutant fibroblasts were isolated directly from E9.5

embryos and maintained at high density in AV3 medium (Dulbecco's modified Eagle's medium supplemented with 15% fetal bovine serum, 1×nucleotides mix, 2mM L-Glutamine, 0.01 mM MEM non essential amino acids and 0.05 mg/ml pen and strep, all from GIBCO). Mutant cell lines were confirmed by PCR genotyping. Fibroblasts were transfected using lipofectamine plus reagent (Invitrogen), following the manufacturer's recommendation. Cells were analyzed 48 hours post-transfection. To immunoprecipitate N-Shhp in the culture medium, we added 30 µl anti-Shh monoclonal antibody 5E1 (DSHB) to 1.5 ml of medium from Shh expressing cells for two hours at 4°C. The antibody and bound proteins were then recovered by overnight incubation with Protein A agarose beads at 4°C. The beads were washed and proteins recovered in sodium dodecyl sulphate-polyacrylamide gel electrophoresis (SDS-PAGE) sample buffer. Biotinylation of cell-surface protein was carried out essentially as described (Denef et al., 2000).

Western blotting

The proteins recovered from Protein A-agarose and streptavidin-agarose beads were separated on a 4-15% SDS-PAGE and transferred to polyvinylidene difluoride (PVDF) membranes for immunoblotting. The membranes were blocked in 5% skimmed milk in PBS with 0.1% Tween 20 (PBST) for 1 hour and incubated with primary antibody against N-Shh (AB80, rabbit polyclonal antibody, 1:1000 dilution) for 1 hour. The membrane was washed three times with PBST, and incubated with secondary antibody (HRP conjugated Donkey anti-rabbit IgG 1:3000 dilution) for 45 minutes, followed by chemiluminescent detection according to the manufacturer's suggestion (Pierce).

Results

A *Disp1* exon 2 deletion allele (*Disp1*$^{\Delta 2}$) is a hypomorphic allele

To determine the role of Disp1 in Hh signaling in mice, we used target mutagenesis in ES cells to generate mice lacking the second exon of *Disp1* (see Fig. S1 at http://dev.biologists.org/supplemental/), a deletion that removes the putative initiation methionine and N-terminal 168 amino acids. Surprisingly, mice homozygous for this allele (*Disp1*$^{\Delta 2/\Delta 2}$) developed to birth. Analysis of *Disp1*$^{\Delta 2}$ transcripts indicated that in the absence of exon 2, exon 1B was replaced by exon 1A, which was subsequently spliced to exon 3, permitting translation from an initiation codon in exon 4 (see Fig. S2 at http://dev.biologists.org/supplemental/). The result was an N-terminal truncated (193aa truncation) Disp1. Hence, the *Disp1*$^{\Delta 2}$ allele probably generates a Disp1 protein that retains most of the membrane spanning and C-terminal regions. In the absence of antibodies that detect the endogenous protein, we have been unable to confirm this prediction.

Disp1$^{\Delta 2/\Delta 2}$ mutants died at birth due to breathing difficulties. All mutants showed mild midline facial defects in which the nose, upper jaw and philtrum were hypoplastic and the eyes were positioned close to the midline (compare Fig. 1A,B,F,G). Examination of the nasal cavity showed a narrowed or closed nasopharyngeal airway with a resulting fusion of the paired, medial-lateral vomeronasal organs (data not shown, and Fig. S3D,E at http://dev.biologists.org/supplemental/). Histological

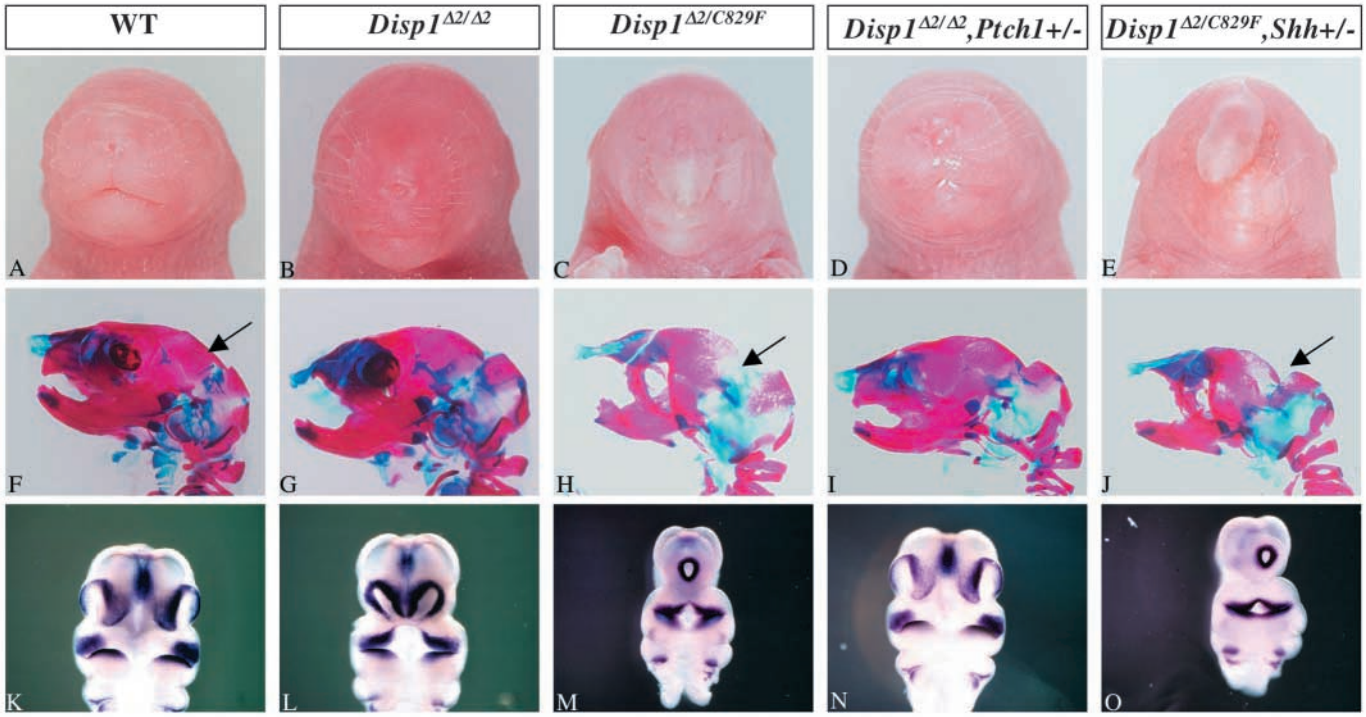

Fig. 1. The *Disp1* gene genetically interacts with Hh-signaling pathway components, including *Ptch1* and *Shh* gene. External facial morphology of E18.5 embryos (A-E). The midline facial defects, clearly visible in *Disp1*$^{\Delta 2/\Delta 2}$ (B), are rescued in *Disp1*$^{\Delta 2/\Delta 2}$, *Ptch1*+/– (D), but exacerbated in *Disp1*$^{\Delta 2/C829F}$ (C), and *Disp1*$^{\Delta 2/C829F}$, *Shh*+/– (E). Alcian Blue- and Alizarin Red-stained skeletons of E18.5 embryos (F-J). The premaxilla and upper incisor are missing from *Disp1*$^{\Delta 2/\Delta 2}$ (G), but restored in *Disp1*$^{\Delta 2/\Delta 2}$, *Ptch1*+/– (I). The premaxilla, upper incisor and parietal bones are missing from *Disp1*$^{\Delta 2/C829F}$ and *Disp1*$^{\Delta 2/C829F}$, *Shh*+/– (H,J). *Fgf8* in situ to demarcate the epithelium of the nasal pit (K-O). Two nasal pits, which are positioned well apart in wild type (K), are brought closer to the midline in *Disp1*$^{\Delta 2/\Delta 2}$ (L), fused in the midline in *Disp1*$^{\Delta 2/C829F}$ (M), and *Disp1*$^{\Delta 2/C829F}$, *Shh*+/– (O), and are separated to normal distance in *Disp1*$^{\Delta 2/\Delta 2}$, *Ptch1*+/– (N).

analysis further revealed midline defects: a loss of the primary palate, upper incisors and pituitary hypoplasia (see Fig. S3). Analysis of *Fgf8* expression, which demarcates the lateral and medial frontal nasal process and maxillary and mandibular epithelium, indicated that midline tissue between these expression domains was absent by E10.5 (Fig. 1K,L). All these defects are characteristic of holoprosencephaly (HPE), which in specific human cases results from reduced Shh signaling in which only one allele is active (reviewed by Wallis and Muenke, 1999).

Disp1$^{\Delta 2}$/*Disp1*^{C829F} mutants exhibited a markedly enhanced facial phenotype, in which there was a further loss of midline structures (Fig. 1C,H): an absence of vomeronasal organ and a failure of pituitary development (Fig. S3). The enhanced midline defects apparent at E10.5 represented a more extreme deletion of midline facial structure (Fig. 1M). In addition, a severe reduction was observed in the parietal bone of the skull (arrow in Fig. 1H). The weak *Disp1*$^{\Delta 2/\Delta 2}$ phenotype and the increased severity of the phenotype on combination of the *Disp1*$^{\Delta 2}$ mutation with the *Disp1*^{C829F} null mutation suggest that *Disp1*$^{\Delta 2}$ generates a hypomorphic allele.

If the midline facial defects reflected reduced levels of available Shh signal, we reasoned that lowering the levels of *Ptch1* may rescue *Disp1*$^{\Delta 2/\Delta 2}$ mice, as Ptch1 sequestration of Hh is known to reduce Hh protein levels in a responding target field (Chen and Struhl, 1996). Indeed, *Disp1*$^{\Delta 2/\Delta 2}$,*Ptch1*+/– mutant pups were viable, fertile and indistinguishable from wild-type littermates (Fig. 1D,I,N). By contrast, reducing Shh levels further might be expected to enhance the midline phenotype. In agreement with this prediction, *Disp1*$^{\Delta 2/C829F}$, *Shh*+/– mutants exhibited an extreme proboscis-like nasal process, the result of a fusion of the lateral frontal nasal processes, a phenotype observed in the most severe forms of HPE and *Shh* null mutants (Fig. 1E,J,O).

The induction of *Shh* and its targets during early forebrain development

Several lines of evidence suggest that the facial anomalies in HPE result from earlier patterning defects in the anterior neural plate (reviewed by Muenke and Beachy, 2000). During early forebrain development, *Shh* is expressed throughout the axial midline mesoderm, underlying the presumptive brain, and its activity is required to induce secondary sites of *Shh* expression in the ventral neural plate (reviewed by McMahon et al., 2003). In *Disp1*$^{\Delta 2/\Delta 2}$ mutants at the 10-somite stage (E8.5), expression of *Shh* in midline mesoderm was comparable to that of wild-type embryos (Fig. 2A,B, arrow). However, only a weak induction of *Shh* was observed at the ventral midline of the midbrain, whereas expression in wild-type embryos extended rostrally into the forebrain and caudally into the hindbrain (Fig. 2A,B, arrowhead). Further, the *Shh*-dependent transcription factors, *Nkx2.1* and *Nkx2.2* (Pabst et al., 2000), which show nested expression domains in the forebrain, were markedly downregulated in *Disp1*$^{\Delta 2/\Delta 2}$ mutants (Fig. 2E,F,I,J). Together, these observations suggest that attenuating Disp1 activity results in markedly reduced Shh-signaling activity during the early stages of forebrain patterning. As a result, target gene activation is more ventrally restricted, suggesting that the strength and range of Shh signaling are both diminished. This is supported by analysis of the expression of the general Hh target gene *Ptch1*, transcription of which provides a direct readout of the range and strength of Hh signaling. In both E8.5 and E9.5 *Disp1*$^{\Delta 2/\Delta 2}$ mutants, *Ptch1* expression was absent in the rostral forebrain and optic stalk and the overall levels of remaining *Ptch1* expression were reduced (Fig. 2M,N and data not shown). When Disp1 or Shh activity was further reduced in *Disp1*$^{\Delta 2/C829F}$ and *Disp1*$^{\Delta 2/C829F}$, *Shh*+/– mutants, respectively, induction of Shh in the midbrain was almost absent, no activation of *Nkx2.1* or *Nkx2.2* were observed in the brain-forming regions of the anterior neural tube and only weak *Ptch1* expression was seen in midbrain and more caudal regions of the neural plate (Fig. 2C,D,G,H,K,L,O,P).

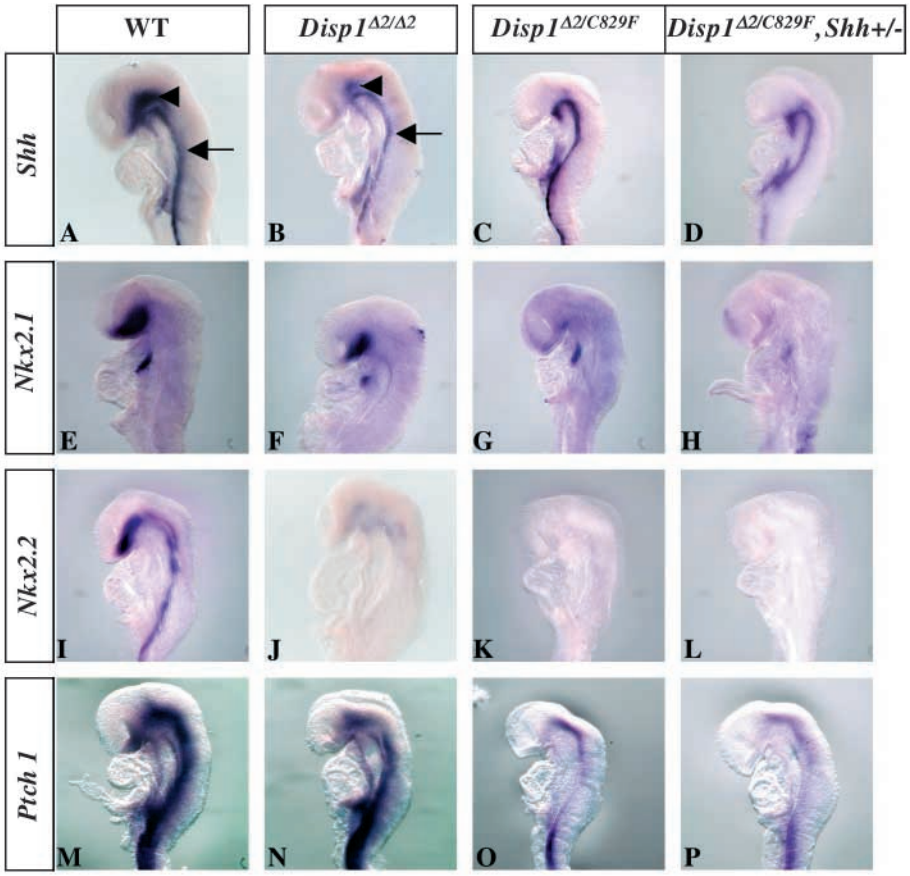

Fig. 2. The induction of *Shh* and its targets at the ventral forebrain is delayed or attenuated at E8.5. Whole-mount in-situ hybridization of *Shh* (A-D); *Nkx2*.1(E-H); *Nkx2.2* (I-L); *Ptch1* (M-P) of E8.5 dpc wild-type and mutant embryos as indicated. Arrow in (A) indicates the *Shh* expression in the axial mesoderm notochord. Arrowhead in (B) indicates expression in the ventral forebrain.

Dorsoventral patterning of the telencephalon is affected in *Disp1* mutants

At E12.5, the ventral (basal) telencephalon is composed of two proliferating cell masses, the medial and lateral ganglionic eminences (MGE and LGE). *Shh* is expressed in ventral telencephalon, primarily in the MGE, preoptic area and prospective amygdala (Rallu et al., 2002). Embryos that lack Shh function fail to form ventral telencephalic structures and to express corresponding markers for the MGE (*Nkx2.1*) and MGE/LGE (pan-ventral genes *Dlx2* and *Mash1*), while the pan-dorsal gene marker (*Ngn2*) spreads ventrally to include the whole telencephalon (Chiang et al., 1996; Rallu et al., 2002). Surprisingly, we failed to observe any detectable alteration in forebrain patterning in $Disp1^{\Delta2/\Delta2}$ mutants, suggesting that while ventral patterning was defective at the 10-somite stage, embryos recovered at later stages (Fig. 3A,B,E,F,I,J,M,N). However, when *Disp1* and *Shh* activity were further reduced, we observed a gradual restriction of pan-ventral genes markers, including *Nkx2.1*, *Mash1* and *Dlx2* to the midline (Fig. 3A-L), and corresponding ventral expansion of pan-dorsal gene *Ngn2* (Fig. 3M-P). Whereas neither the LGE nor MGE is readily morphologically identifiable, regional marker analysis indicated that some MGE (*Nkx2.1*) cells were present in the $Disp1^{\Delta2/C829F}$ mutant, but none were present in the $Disp1^{\Delta2/C829F}$, *Shh*+/– mutant, where the residual domain of *Mash1*- and *Dlx2*-expressing cells presumably reflects a markedly reduced LGE (Fig. 3G,H,K,L). Together, these results indicate that *Disp1* and *Shh* genetically interact to coordinate patterning of the MGE and LGE, and that a progressive reduction of Shh signaling activity, by reducing Disp1 and Shh levels, leads to a progressive increase in the severity of the loss of ventral neural progenitors.

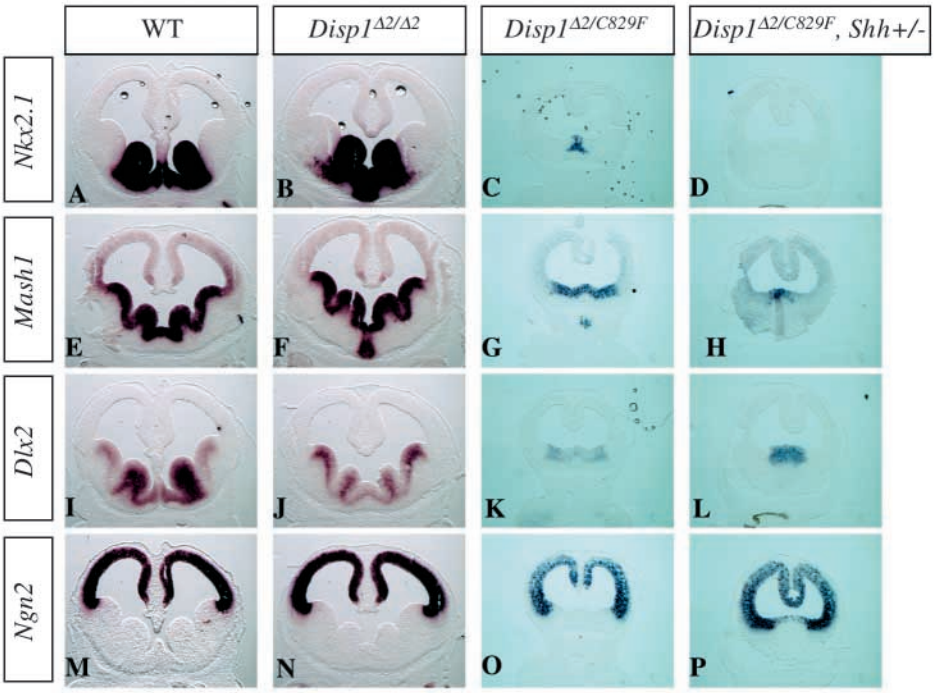

Fig. 3. Dorsoventral patterning of telencephalon is affected in *Disp1* mutants. Coronal sections of E12.5 embryo of wild type, $Disp1^{\Delta2/\Delta2}$, $Disp1^{\Delta2/C829F}$, and $Disp1^{\Delta2/C829F}$, *Shh*+/– were assayed for expression of region-specific homeobox gene *Nkx2.1* (A-D), *Mash1* (E-H), *Dlx2* (I-L) and *Ngn2* (M-P). Progressive attenuation of Shh-signaling strength through genetic manipulation of *Disp1* and *Shh* genes leads to gradual restriction of Pan-ventral gene markers, including *Nkx2.1*, *Mash1* and *Dlx2*, to the midline; and corresponding expansion of Pan-dorsal gene *Ngn2*.

Absence of floor plate, reduction of ventral neural progenitor population and expansion of dorsal neural precursors in response to attenuated Shh signaling

Embryos with attenuated *Disp1* function also display patterning defects at more caudal levels. The ventral half of the neural tube is occupied by five progenitor populations, which consist of, from ventral to dorsal, pV3, pMN, pV2, pV1 and pV0 in the medial ventricular zone. These cells move laterally and differentiate into V3 interneurons, motoneurons, and V2, V1, V0 interneurons, respectively (reviewed by Briscoe and Ericson, 2001; Jessell, 2000). Many lines of evidence indicate that dose-dependent Shh signaling, initially by the notochord and later by the ventral midline floor plate cells, plays a central role in the induction of these cell types (reviewed by Briscoe and Ericson, 2001; Jessell, 2000; McMahon et al., 2003). A key aspect of these inductive events is that from pV0 to the floor plate, individual cell identities require a progressively higher concentration of Shh for their induction, with the highest level required for the induction of Shh-expressing ventral midline floor plate cells, an event that is normally contact-dependent (Placzek et al., 1990).

To investigate ventral patterning defects in *Disp1* mutants, we looked at the expression of Class I and Class II homeobox proteins that distinguish distinct classes of neural progenitors (reviewed by Briscoe and Ericson, 2001; Jessell, 2000). Class I genes (*Dbx1*, *Dbx2*, *Pax6*, *Pax3* and *Irx3*) are repressed while Class II genes (*Nkx2.2*, *Nkx6.1* and *Olig2*) are activated at different concentration thresholds of Shh. The ventral boundaries of Class I and dorsal boundaries of Class II genes demarcate neural progenitor domains within the ventral half of the neural tube. As with the forebrain, we observed a progressive (ventral to dorsal) loss of ventral progenitor population that correlated with the increasing severity of the *Disp1* and *Shh* mutant alleles. When $Disp1^{\Delta2/\Delta2}$ hypomorphic embryos were examined, the floor plate markers (*HNF3β* and *Shh*) were not induced at the medial ventral neural plate (Fig. 4A,E). The midline was occupied by $Nkx2.2^{+}$ pV3 progenitors ($Disp1^{\Delta2/\Delta2}$, 24±6, n=5), whose numbers were only 40% of wild-type control (wt, 60±6, n=5, P<0.01) (Fig. 4B,F,U,V). When Disp1 levels were further reduced in $Disp1^{\Delta2/C829F}$ embryos, we observed a further reduction in pV3

(*Disp1*$^{\Delta 2/C829F}$, 7±3 *n*=5) progenitors (Fig. 4I,J,U,V). An additional reduction of Shh-signaling strength in *Disp1*$^{\Delta 2/C829F}$, *Shh*+/– mutant led to the complete loss of the pV3 progenitors (Fig. 4M,N,U,V). The ventral midline was now occupied by a reduced population of pMN cells (wt, 71±6, *Disp1*$^{\Delta 2/C829F}$, *Shh*+/–, 5±2, *n*=5, *P*<0.01) (Fig. 4N,V). The domain occupied by Nkx6.1-producing cells (wt, 175±15, *n*=5) was also reduced in the hypomorphic mutants *Disp1*$^{\Delta 2/\Delta 2}$ (125±10), *Disp1*$^{\Delta 2/C829F}$ (60±5), and *Disp1*$^{\Delta 2/C829F}$, *Shh*+/– (63±5, *n*=5, *P*<0.01) (Fig. 4C,G,K,O,W). As Nkx6.1 demarcates pV3, pMN and pV2 progenitors, the results suggest that even in the most severe mutants, Shh-signaling levels are sufficient to induce pV2 progenitors, and pV2 progenitors expand ventrally on reduction of *Disp1* activity. In general, we observed a graded increase in severity of the observed phenotypes with increasing severity of the allelic combinations (floor plate>pV3>pMN>pV2), that mirrors the in-vitro dependence of a given progenitor population on an increasing concentration of Shh for induction (FP>pV3>pMN>pV2) (Roelink et al., 1995; Ericson et al., 1997a).

Expression of *Pax6*, a class I gene, shifted ventrally, but a sharp boundary between Nkx2.2^{+} and Pax6^{+} was still maintained in *Disp1* mutants (Fig. 4D,H,L,P,T). *Pax7*, the dorsalmost Class I gene, was expressed more ventrally, but its expression domain was maintained dorsal to that of *Nkx6.1* (Fig. 4C,G,K,O). Together these results indicate that low-level Shh signaling occurs, but at a relatively more ventral position in *Disp1* mutants.

The severe reduction of the pMN neural progenitor population translated to a significant decrease in MNR-positive motoneuron precursors that were abnormally positioned, occupying the ventral midline in all mutants (wt, 145±15, *Disp1*$^{\Delta 2/\Delta 2}$, 98±14, *Disp1*$^{\Delta 2/C829F}$, 80±10, *Disp1*$^{\Delta 2/C829F}$, *Shh*+/–, 73±6, *n*=5, *P*<0.01) (Fig. 5A,E,I,M). Chox10^{+} V2, En1^{+} V1 and Evx1/2^{+} V0 interneuron precursors were present in approximately normal numbers, but there was a higher degree of mixing between these populations, and a ventral progression of their domains that correlated with the severity of the allelic combinations (Fig. 5B,F,J,N). As expected, we also observed an accompanying ventral shift in *Lim1/2* expression, a regulatory factor that is present within V0, V1 and V2 precursors, and D5 dorsal precursors that derive from dorsal pD5 progenitors.

Consistent with the view that reduced Shh signaling underlies the CNS patterning defects in *Disp1*$^{\Delta 2/\Delta 2}$ mutants, the floor plate was restored and progenitor/precursors cells were induced at the correct

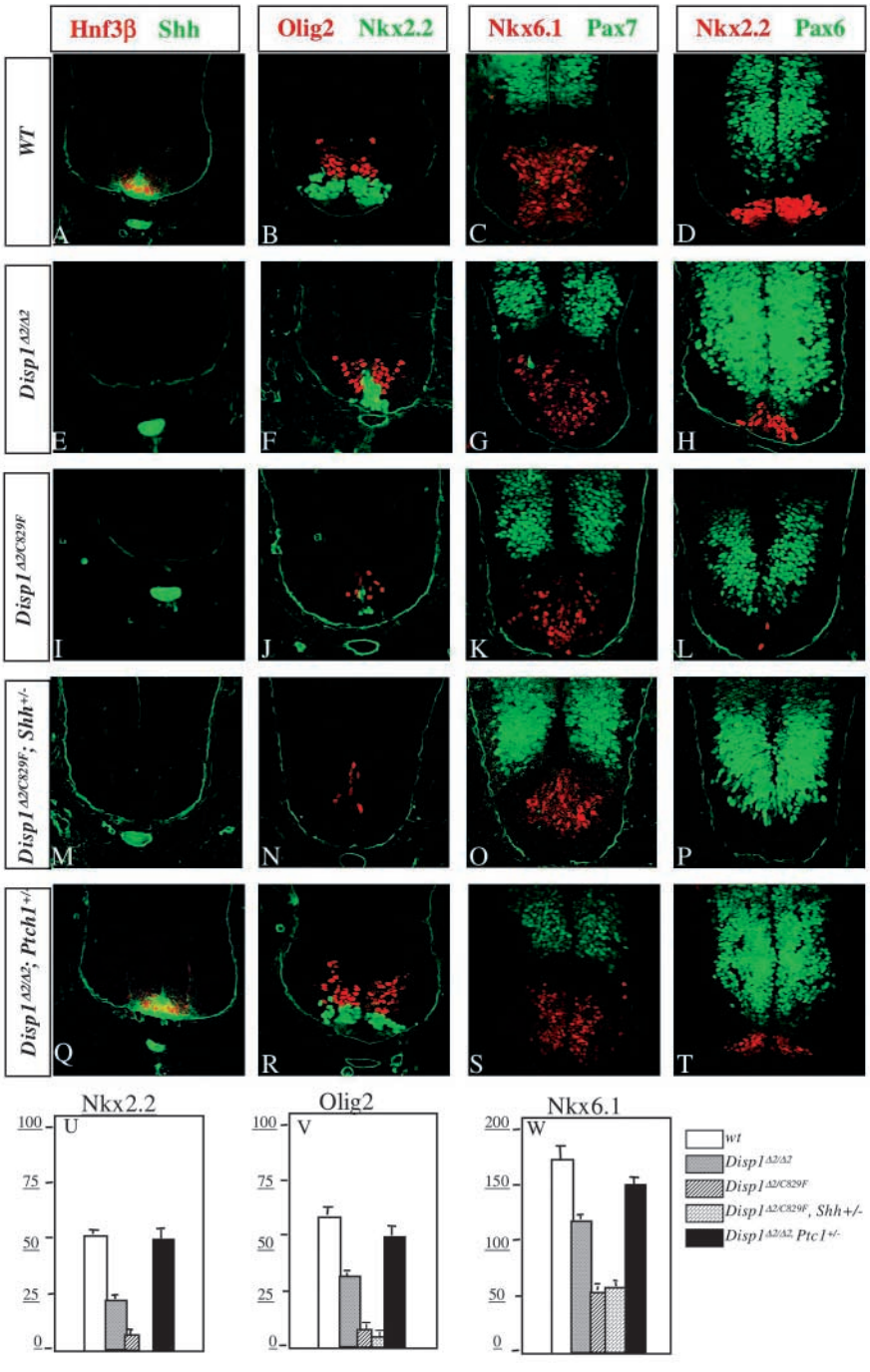

Fig. 4. Absence of floor plate, reduction of ventral neural progenitor population in response to attenuated Shh signaling in Disp1 hypomorphic mutants. Sections through the neural tube of control (A-D), *Disp1* hypomorphic mutants (as indicated). In *Disp1*$^{\Delta 2/\Delta 2}$ mutant (E-H): the floor plate is absent (E); Nkx2.2 and Olig2 positive cells are reduced by over 50% (F); Nkx2.2 cells occupy the ventral midline (F); and Nkx6.1-positive cells are also affected (G). The dorsal marker Pax7 is restricted to the dorsal domain (G). In *Disp1*$^{\Delta 2/C829F}$ mutant (I-L), both Nkx2.2 and Olig2 are further reduced (J). The Pax7 and Pax6 domains move ventrally (K,L). In *Disp1*$^{\Delta 2/C829F}$, *Shh*+/– mutant (M-P), Nkx2.2-positive cell is absent (N). Reducing the sequestration by *Ptch1* rescues the *Disp1*$^{\Delta 2/\Delta 2}$ spinal cord phenotype in *Disp1*$^{\Delta 2/\Delta 2}$, *Ptch1*+/– mutant (Q-T).

position and in comparable numbers with wild-type embryos on removal of a single allele of *Ptch1* (Fig. 4Q-T, Fig. 5Q-T). In summary, the observed phenotype in *Disp1* mutants provides strong evidence for a role in regulating the levels of Shh that are made available to the neural target field by the underlying notochord.

Skeletal patterning defects in *Disp1* mutants

hedgehog signaling plays several distinct roles in skeletal patterning. Initially, Shh signaling from midline (notochord and floor plate) induces sclerotome formation in the adjacent ventral somite (Fan et al., 1995). Sclerotome precursors then generate the axial skeleton. Both the axial and appendicular skeleton requires Ihh signaling to regulate proliferation and differentiation of skeletal progenitors (reviewed by McMahon et al., 2003). By contrast to *Disp1* null mutants that fail to express ventral somite markers prior to developmental arrest (Caspary et al., 2002; Kawakami et al., 2002; Ma et al., 2002), $Disp1^{\Delta 2/C829F}$ embryos form a relatively normal axial and appendicular skeleton, the only difference from wild-type being a slight delay in chondrocyte differentiation at cervical levels (data not shown). However, various deficiencies were apparent in the head skeleton (Fig. 6A,B,C,D,E,F). As expected from the loss of facial progenitors between the frontal nasal processes that accompanies the midline defects in the $Disp1^{\Delta 2/C829F}$ ventral forebrain, $Disp1^{\Delta 2/C829F}$ embryos displayed a dramatic loss of premaxillary frontal nasal components, including the primary palate and upper incisor, which are all derived from the neural crest (Fig. S3). In addition, we observed a complete absence of the parietal bone, whereas the basisphenoid and occipital bones (supra-, ex-, basi-) are either misshapen or reduced in size (Fig. 6E,F). Thus, the data suggest that the anterior paraxial mesoderm of the cephalic skeleton from which these bones derive is relatively more sensitive to *Disp1* function than more caudal somitic regions.

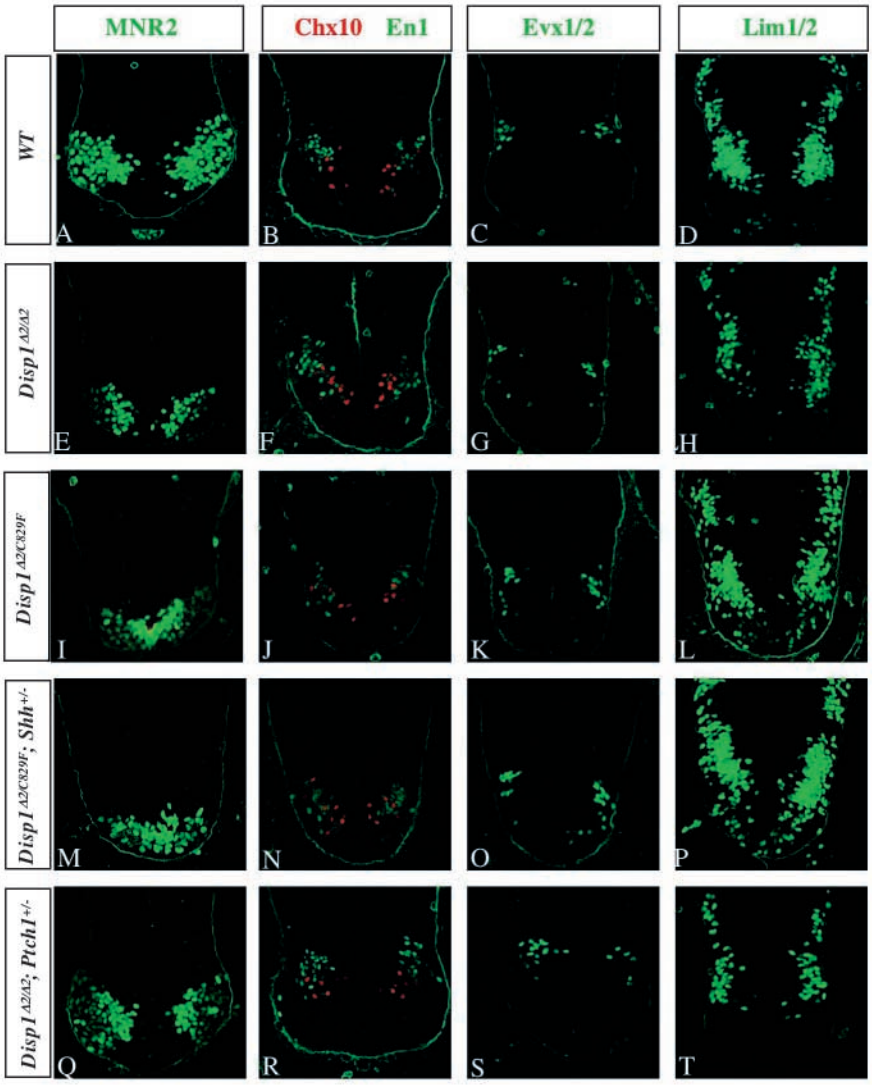

Fig. 5. Ventral neural precursor patterning defects in *Disp1* hypomorphic mutants. Motoneuron precursors (MNR^+ cell) occupy the ventral midline in $Disp1^{\Delta 2/C829F}$ (I) and $Disp1^{\Delta 2/C829F}$, *Shh*+/– mutants (M), instead of its normal lateral position in wild type (A). V2 ($Chox10^+$) and V1 ($En1^+$) interneurons are present in comparable numbers in *Disp1* mutants as the wild type (B,F,J,N). V0 ($Evx1/2^+$) precursors expand ventrally in *Disp1* mutants (C,G,K,O). Lim1/2-positive cells, which demarcate the p5, V0 and V1 precursor populations also expand ventrally in *Disp1* mutants (D,H,L,P).

The genetic mechanisms that pattern the cranial paraxial mesoderm are rather poorly understood. Analysis of expression profiles from *Shh* mutants has identified a number of genes whose activity correlates with skeletal development (T.T. and A.P.M., unpublished data). *FoxD1* and *FoxD2* were expressed in mesenchymal precursors in the head adjacent to ventral brain regions and their expression was markedly downregulated in $Disp1^{\Delta 2/C829F}$ mutants at E9.5 (arrow in Fig. 6G-J). Thus, the down regulation of these genes within the cephalic mesenchyme correlates with the skeletal defects observed in $Disp1^{\Delta 2/C829F}$ mutants. *FoxD1* and *FoxD2* expression was also lost where midline facial mesenchyme was missing (arrowhead in Fig. 6G-J).

Disp1 is involved in *Ihh* signaling

Disp1 null mutants arrest early with L-R patterning defects that resemble those observed in both *Smo* and *Shh/Ihh* compound mutants (Chiang et al., 1996; St-Jacques et al., 1999; Zhang et al., 2001b). Thus, it has been proposed that Disp1 plays a similar essential role in both Shh and Ihh signaling (Kawakami et al., 2002; Ma et al., 2002). To investigate this possibility, we compared the phenotype of *Shh*–/– and $Disp1^{\Delta 2/C829F}$, *Shh*–/– mutants at E9.5. Whereas *Shh*–/– embryos undergo heart looping, albeit randomized due to the loss of a midline barrier (Fig. 7A,B) (Meyers and Martin, 1999), $Disp1^{\Delta 2/C829F}$, *Shh*–/– embryos fail to undergo heart looping. Interestingly, these

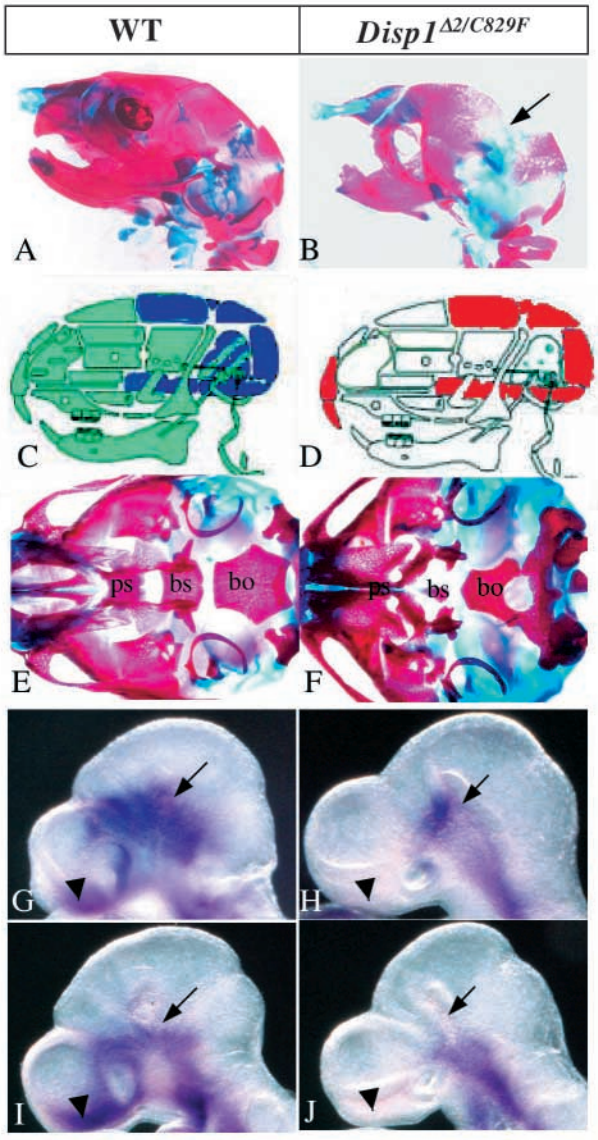

Fig. 6. Cephalic mesoderm patterning is affected in *Disp1*$^{\Delta 2/C829F}$ mutants. (A-B) Alcian Blue- and Alizarin Red-stained skull from E18.5 dpc embryos. (C) Model of skeletal elements of the vertebrate skull. Elements formed by neural crest are labeled green and those by mesoderm are labeled purple. (D) Skull elements altered in *Disp1*$^{\Delta 2/C829F}$ mutants are highlighted in red, which overlap with most of the skeletal elements with mesoderm origin. (E,F) Ventral view of the base of the brain; note that the basioccipital bone (bo) and basisphenoid bones (bs) are misshapen and greatly reduced in *Disp1*$^{\Delta 2/C829F}$ mutant. Whole-mount in-situ hybridization of paraxial mesoderm markers *FoxD1* (G,H), *FoxD2* (I,J) show clear reduction in the cephalic mesoderm area in *Disp1*$^{\Delta 2/C829F}$ mutant.

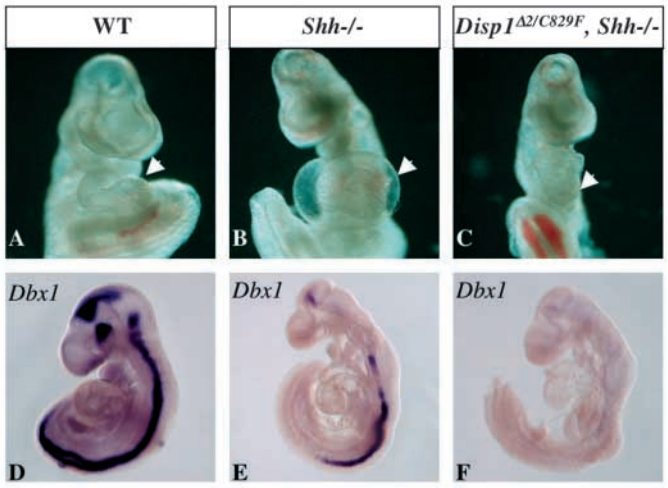

Fig. 7. *Disp1* genetically interacts with *Ihh* signaling at the early stage of embryonic development from E7.5 to 9.5. External morphology of E9.5 dpc embryos: (A) wild type; (B) *Shh*–/–; (C) *Disp1*$^{\Delta 2/C829F}$, *Shh*–/–. Heart looping is clearly visible in wild-type (A) and *Shh*–/– (B) mutant. No heart looping occurs in *Disp1*$^{\Delta 2/C829F}$, *Shh*–/– (C). Whole-mount in-situ of *Dbx1* expression in wild type (D), *Shh*–/– (E) and *Disp1*$^{\Delta 2/C829F}$, *Shh*–/– (F).

mutants do undergo embryonic turning. So in this mutant combination, heart looping and turning, both of which are distinct aspects of L-R asymmetry, are genetically separable. Thus, the *Disp1*$^{\Delta 2/C829F}$ alleles enhance the *Shh* null phenotype, consistent with an additional role for Disp1 in Ihh signaling. Further evidence to support this conclusion comes from analysis of the expression of *Dbx1*. Normal *Dbx1* expression in p0 progenitors is dependent on hedgehog signaling (Wijgerde et al., 2002). Further, the presence of some ventral *Dbx1* expressing cells in *Shh* mutants suggests a role for Ihh signaling in maintaining residual expression (Wijgerde et al., 2002) (Fig. 7D,E). However, when *Disp1* activity was decreased in *Disp1*$^{\Delta 2/C829F}$, *Shh*–/– embryos, all *Dbx1* expression was lost, suggesting that residual Ihh signaling is reduced to sub-threshold levels (Fig. 7F). Given these results, it is therefore surprising that by contrast to the marked skeletal defects that result from perturbation of Ihh signaling (St-Jacques et al., 1999), *Disp1*$^{\Delta 2/C829F}$, *Ihh*+/– mutant embryos, although slightly smaller than wild-type littermates at birth, display a wild-type organization of the endochondral skeleton (data not shown).

Disp1 topology, subcellular distribution, and role in hedgehog trafficking and release

Disp1 is predicted to encode a multipass transmembrane protein (Fig. 8A). To address the orientation of Disp1 within the membrane, we used N-terminal (DspN) and C-terminal (DspC) domain-specific anti-Disp1 antibodies for immunofluorescent staining of Disp1 in permeabilized and non-permeabilized cells. No staining was observed in transfected non-permeabilized cells with either antibody or with antibodies that recognize specific proteins within the secretory pathway, including ER-specific molecular chaperone heavy chain binding protein (BIP) and Golgi matrix protein (GM130) (Fig. 8B). By contrast, AB80 antibody, which recognizes N-Shh, displayed a clear cell-surface staining in cells transfected with a full-length Shh expression construct. However, immunostaining of both the N- and C-terminal domain antibodies and control BIP/GM130 antibodies was observed in permeabilized cells (Fig. 8B). Thus, both the N- and C-terminal domains are cytoplasmic, which leads us to propose a topological model in which Disp1 contains 12 TM domains with a cytosolic amino terminus and carboxy-terminal

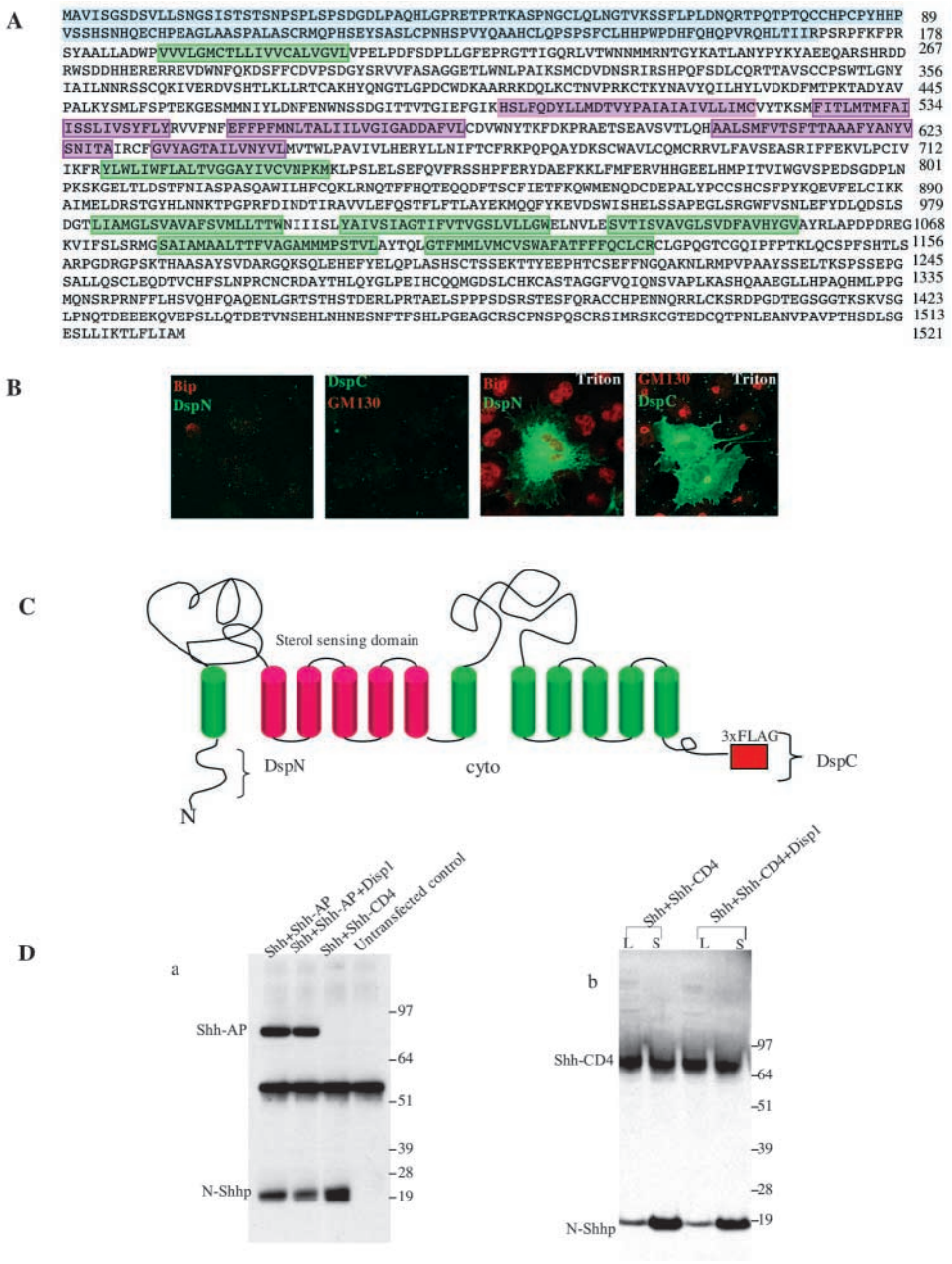

Fig. 8. Analysis of Disp1 topology, localization and role in Shh secretion. (A) The predicted sequence of Disp1, with transmembrane helix highlighted in green and red. The blue-shaded sequence indicates what has been deleted in *Disp1*$^{\Delta 2}$ mutation. (B) No signal was detected by immunostaining on unpermeabilized Cos7 cell using DspN and DspC antibodies. After permeabilization with Triton, Disp1 immunostaining were co-localized with ER marker Bip, and Golgi marker GM130. The protein also displayed a typical cell-surface distribution. (C) Proposed topology of Disp1 with sterol-sensing domain highlighted in red. (D) Immortalized *Disp1*$^{C829F/C829F}$ mutant fibroblast was transfected with expression constructs as indicated (a). After 2 days, the media were collected and Shh protein was immuno-pulled down with anti-Shh 5E1 monoclonal antibody, separated by SDS-PAGE, and immuno-detected with anti-Shh AB80 polyclonal antibodies. (b) Cell-surface proteins were labeled by biotin and pulled down by streptavidin, then separated by SDS-PAGE and immuno-detected with AB80. L, cell lysate input before biotinylation; S, cell-surface fraction pulled down with streptavidin.

tail (Fig. 8C). This configuration places the sterol-sensing domain of Disp1 in the same orientation as the homologous domains within SCAP and NPC1. High resolution imaging of a Disp1-EYFP fusion indicated a punctate membrane localization, with a preferred basal-lateral distribution, in polarized epithelial Madin-Darby canine kidney (MDCK) cells (data not shown).

One mechanism by which Disp1 might regulate available hedgehog signals is to regulate release of lipid-modified ligands from producing cells (Burke et al., 1999; Ma et al., 2002). To examine this issue, we generated immortalized *Disp1*$^{C829F/C829F}$ fibroblast cell lines from E9.0 mutant embryos. When *Disp1*$^{C829F/C829F}$ mutant cells were transfected with Shh, significant amounts of processed Shh-Np (19K) were immuno-precipitated from culture medium by anti-Shh 5E1 monoclonal antibody (Fig. 8Da). To quantify the amount of Shh released in the presence or absence of the Disp1 gene (introduced by co-transfection), we co-transfected a full-length Shh gene with a second construct that encodes a secreted Shh-AP fusion protein, where the N-terminal signaling domain of Shh is fused in frame at its N-terminus with alkaline phosphatase (Chuang and McMahon, 1999). Shh-AP (MW 71 kDa) can be efficiently secreted into the medium and pulled down from the culture medium by anti-Shh antibody; thus, it serves as an internal control for transfection efficiency. After normalizing for the Shh-AP signal density, no difference was observed in N-Shhp accumulation in the medium in either the presence or absence of Disp1. The expression of Disp1 in these experiments was confirmed by Western blotting using antibody against a FLAG tag fused at the C-terminal end of Disp1 protein (data not shown). The absence of detectable levels of a membrane bond Shh-CD4 (M_r 86 kDa) fusion protein in the culture medium indicates that the accumulation of N-Shhp and Shh-AP proteins in the medium was not caused by cell lysis (Fig. 8Da).

Next, we examined the cell-surface accumulation of Shh protein in *Disp1*$^{C829F/C829F}$ mutant fibroblasts. All cell-surface proteins were labeled with biotin and precipitated with streptavidin conjugated beads and separated by SDS-PAGE. The absence of ER protein BIP, Golgi protein GM130, as well as the full-length unprocessed Shh precursor in the pull-down

fraction indicated that biotin labeling was specific for cell-surface proteins (data not shown). We co-transfected a transmembrane anchored Shh, Shh-CD4 (M_r 86 kDa), as a control for normalization of transfection efficiency (Fig. 8Db). Shh-CD4 can be labeled and pulled down effectively by streptavidin beads, in a similar way to N-Shhp. We detected only processed forms of N-Shhp on the cell surface, further evidence that the pulled-down components were from intact cells. After normalization for Shh-CD4 levels, Shh-Np accumulation on the cell surface, as well as in the cell lysate, showed no difference in the presence or absence of Disp1 in *Disp1*$^{C829F/C829F}$ mutant fibroblasts. Again, the presence of full-length Disp1 in this experiment was confirmed by Western blot analysis (data not shown).

Ma et al. (Ma et al., 2002) have reported that Disp activity in *Drosophila* S2 cells increases the extracellular export of a Shh::Renilla luciferase fusion protein. We investigated production and secretion of Shh::luciferase in the presence or absence of *Disp1* in mouse fibroblasts. However, we observed almost no normal processing of the Shh::luciferase precursor, which therefore precluded any further analysis (data not shown). In agreement with the observations of Ma et al. (Ma et al., 2002), co-culture of a Shh reporter cell line with fibroblast cells expressing Shh in the presence or absence of *Disp1* led to a modest (1.25 fold) *Disp1*-dependent increase in signaling activity in reporter cells (data not shown).

Discussion

Early studies have established that mouse embryos lacking Disp1 activity die at E9.5, with phenotypes nearly identical to the *Smo*–/– mutant (Caspary et al., 2002; Kawakami et al., 2002; Ma et al., 2002), suggesting a complete loss of Hh signaling during early embryonic development, except for the autocrine signaling within the notochord (Caspary et al., 2002; Ma et al., 2002). However, the severity of this phenotype precludes a detailed analysis of the genetic interaction between *Disp1* and other Hh-signaling-pathway components. In this study, we took advantage of a new allele of mouse *Dispatched1*, *Disp1*$^{\Delta 2}$. Several lines of evidence indicated that *Disp1*$^{\Delta 2}$ encodes a hypomorphic allele. First, *Disp1*$^{\Delta 2}$ deleted a small region of N-terminal sequence that includes the normal initiation methionine. However, the presence of a downstream ATG with a good Kozak consensus sequence probably enabled production of a new protein that lacks the N-terminal cytoplasmic domain of Disp1. Second, the *Disp1*$^{\Delta 2/\Delta 2}$ phenotype was significantly weaker than that described for other putative null alleles, and intercrossing the *Disp1*$^{\Delta 2}$ allele with one of these probable null alleles *Disp1*^{C829F} resulted in an intermediate phenotype more severe than *Disp1*$^{\Delta 2/\Delta 2}$ but less severe than *Disp1*$^{C829F/C829F}$ homozygous embryos. Thus, by analyzing allelic combination of *Disp1* together with mutant alleles for *Shh*, *Ihh* and *Ptch1*, we have been able to explore the genetic interactions between these hedgehog pathway components in the mammalian embryo.

Disp1 in head and axial skeletal development

Attenuated Hh signaling, for example where one allele of Shh is inactive, has been linked to midline facial defects that characterize HPE (for a review, see Muenke and Beachy, 2000). In comparison with other Hh-dependent signaling events, facial development appears to be consistently more sensitive to attenuation of Hh-ligand concentration or Hh-signaling strength. The loss of midline facial structures and the associated ventral displacement of the eyes are all thought to result from an initial perturbation in midline patterning of the ventral forebrain. In the present study, we observed a relatively mild HPE phenotype in *Disp1*$^{\Delta 2/\Delta 2}$ mutants that increased in severity in *Disp1*$^{\Delta 2/C829F}$ embryos. When Shh dosage was decreased, *Disp1*$^{\Delta 2/C829F}$, *Shh*+/– embryos exhibited a further enhanced HPE with a proboscis nose that closely resembled the most severe facial phenotype of *Shh*–/– mutant embryos (Chiang et al., 1996). A simple explanation for the observed interaction between *Disp1* and *Shh* is that Disp1 regulates Shh signaling and that Shh-signaling activity is sensitive to Disp1 levels. The observed facial phenotypes probably arise secondary to defective ventral forebrain patterning and the associated reduction in ventral forebrain-derived Shh. As *Disp1* and *Shh* activity were progressively reduced, we observed an increasingly more severe failure in the induction of *Nkx2.1*- and *Nkx2.2*-expressing ventral forebrain cell identities that are dependent on mesendoderm-derived Shh signaling, despite normal *Shh* expression in the mesendoderm (Muhr et al., 1997; Pabst et al., 2000). Since Shh induces its own expression in the ventral forebrain, and ventral forebrain-derived Shh is essential for facial patterning (Hu and Helms, 1999), reduced *Shh* expression from this site probably plays a substantial role in the generation of the observed facial phenotypes.

In addition to the loss of midline neural crest-derived structures, the parietal bone was absent and several other bones that arise from the cephalic paraxial mesoderm were reduced or misshapen in *Disp1*$^{\Delta 2/C829F}$ mutants. To date, there is little information on patterning of the cephalic mesoderm. Our evidence suggests that Shh signaling is likely to play an important role, and the reduced expression of two highly related Fox family members in this region, *FoxD1* and *FoxD2*, implicates these factors in the patterning process. The lack of an obvious head skeletal phenotype in either single *FoxD* mutant may reflect redundant roles for these closely related forkhead genes (Hatini et al., 1996; Kume et al., 2000).

Surprisingly, although a considerable body of evidence indicates that Shh signaling plays a central role in the initial step of axial skeleton development and sclerotome induction in the paraxial mesoderm of the trunk, somites (reviewed by McMahon et al., 2003) and vertebrae form normally in the most extreme mutant combinations examined (*Disp1*$^{\Delta 2/C829F}$, *Shh*+/–). That Disp1 is required for sclerotome induction is evident from analysis of *Disp1* null mutants (Caspary et al., 2002; Kawakami et al., 2002; Ma et al., 2002). Thus, it is likely that low levels of Shh signaling suffice for sclerotomal patterning; a view consistent with in-vitro inductive assays of muscle and sclerotome patterning in the zebrafish (Hammerschmidt et al., 1996).

Disp1 and spinal cord patterning

Arguably the best-characterized Hh target field with respect to the issue of dose-dependent Hh signaling is the ventral spinal cord. As expected from current models, the first cell identity that is expected to be lost as Shh signaling is reduced is the midline floor plate. In vitro, floor plate induction requires the highest Shh concentration threshold (Ericson et al., 1997a). In

vivo, notochord transplants indicate that floor plate induction by the notochord is contact-dependent (Placzek et al., 1990), consistent with an inductive event that may utilize concentration thresholds in vivo that are only possible on the cell surface. *Disp1*$^{\Delta 2/\Delta 2}$ mutants fail to undergo floor plate induction; they also exhibit reduced numbers of pV3 interneuron progenitors, the cell identity with the next highest concentration requirement for Shh in vitro (Ericson et al., 1997a). By contrast, all other ventral cell identities are present at approximately wild-type levels, a phenotype that closely resembles loss of *Gli2*, a transcription effector of Shh signaling in the ventral neural tube (Ding et al., 1998; Matise et al., 1998). pV3 progenitors are entirely lost when Shh signaling is further attenuated in *Disp1*$^{\Delta 2/C829F}$, *Shh*+/– mutants, and pMN progenitor populations, that require the next highest level of Shh input in vitro, are markedly reduced. In summary, both the morphological and molecular analysis link *Disp1* to the Shh pathway, and the range of phenotypes we observe are completely consistent with the view that *Disp1* dosage regulates the level of hedgehog signaling in target tissues.

Disp1 action

In principle, Disp1 may regulate hedgehog signaling in either the producing or responding cell. *Drosophila* studies indicate that Disp is required only in Hh-producing cells (Burke et al., 1999). In the mouse, the persistence of Shh signaling in the notochord of *Disp1*$^{C829F/C829F}$ mutants, in which cells both produce and respond to ligands, suggest that in this auto-regulatory loop, Disp1 is not essential for transducing an Shh signal where autocrine signaling is likely to be occurring (Caspary et al., 2002; Ma et al., 2002).

Previous studies in *Drosophila* and mouse cells have demonstrated that translation and processing of hedgehog ligands are unchanged in *disp* or *Disp1* mutants (Burke et al., 1999; Kawakami et al., 2002; Ma et al., 2002). Disp1 must regulate Shh availability by some other mechanism. Several possible roles can be imagined: (1) Disp1 may be involved in intracellular trafficking of Hh to the cell surface; (2) it may regulate direct release of Hh protein into the extracellular space; or (3) it may facilitate the effective surface presentation of Hh to adjacent receiving cells. To distinguish between these possibilities, we derived fibroblast cultures from *Disp1*$^{C829F/C829F}$ embryos and gauged the levels of cell surface-accumulated and medium-accumulated Hh protein.

First, accumulation of Shh on the surface of fibroblasts in culture was not affected by the absence of Disp1. Whether fibroblasts and epithelial cells differ in this regard is unclear. For example, a recent in-vivo study suggests that *disp* is involved in regulating apical-specific accumulation of Hh in the *Drosophila* epidermis, an issue that cannot be examined in a non-epithelial fibroblast line (Gallet et al., 2003). We also failed to observe any role for Disp1 in secretion of Shh into the medium in fibroblast cell culture. Thus, the Shh secretion we observed in vitro is Disp1 independent; the fact that there is little or no response in Hh target fields of *Disp1*^{null} embryos (Caspary et al., 2002; Kawakami et al., 2002; Ma et al., 2002) suggests that this form of secretion is not likely to play a significant role in vivo. However, the secreted N-Shhp from Disp1 null fibroblasts is biologically active, as demonstrated by its ability to activate alkaline phosphatase activity in C3H10T1/2 cells (data not shown). Interestingly, the existence of a Disp-independent release (default release) of Hh protein has been demonstrated in the *Drosophila* epidermis, where Hh retains the ability to travel to adjacent receiving cells and elicit downstream signaling events in cells posterior to the Hh-expressing domain in *disp* mutants (Gallet et al., 2003). Thus, our studies argue against a simple model in which Disp1 only regulates release of Shh into the extracellular space and in so doing, signals in the target field. For example, Disp1 may be involved in efficiently presenting Hh ligand to a specific mediator, which then relays Hh ligand to the target field.

By contrast to our findings, a role for Disp1 in Shh secretion from cells has been suggested from other lines of experiment. Ma et al. (Ma et al., 2002) reported that when Shh-expressing *Disp1*–/– mutant fibroblasts were mixed with an Shh-responsive cell line, overexpressing Disp1 in these cells leads to 1.6-fold increase in Hh-dependent response, suggestive of increased ligand levels. We observed a similar low level of increase in the same assay (1.25-fold, data not shown). Given that our results indicate that there is no change in the bulk level of secreted Shh protein in the presence or absence of Disp1 in vitro, the slight increase in activity may reflect a minor component of this fraction, for example, in a more active oligomeric complex (Zeng et al., 2001). Elevated Disp1 levels in *Drosophila* S2 cells were reported to enhance accumulation of a Shh::Renilla luciferase fusion protein in the medium (Ma et al., 2002). However, we were unable to verify this result in mouse fibroblasts, because this fusion protein fails to undergo efficient processing. At present, the specific action of Disp1 remains unclear.

Does Disp1 function exclusively in the Hh pathway in vertebrates, as appears to be true for its *Drosophila* counterpart (Burke et al., 1999)? A key piece of evidence in support of this view comes from analysis of *Disp1*$^{\Delta 2/\Delta 2}$, *Ptch1*+/– mutants, in which reducing *Ptch1* dosage completely rescues the *Disp1*$^{\Delta 2/\Delta 2}$ phenotype. Ptch1 plays two key roles in hedgehog signaling (reviewed by Ingham and McMahon, 2001): inhibiting Smoothened activation of hedgehog targets and sequestering Hh ligand in negative feedback control. Thus, either sensitizing the initial Hh induction, or increasing available ligand by attenuating the feedback loop, is sufficient to compensate for decreased Disp1 activity and the resulting decrease in Shh signaling.

Does Disp1 play an equivalent role in signaling by other mammalian hedgehog ligands? As *Dhh* phenotypes are most apparent in neonatal and adult mice and *Disp1*$^{\Delta 2/C829F}$ mutants die at birth, we focused our studies on *Ihh*. The strong resemblance of *Disp1* null mutants to *Shh/Ihh* compound mutants, which also arrest at E9.5, favors the view that Disp1 mediates both Shh and Ihh signaling (Caspary et al., 2002; Kawakami et al., 2002; Ma et al., 2002). In agreement with a Disp1 role in Ihh signaling in the early somite embryo, *Dbx1* expression in the ventral neural tube of *Shh*–/– embryos, which probably depends on residual Ihh signaling (Zhang et al., 2001b), was completely lost when Disp1 activity was reduced in *Disp1*$^{\Delta 2/C829F}$, *Shh*–/– embryos. Later in development, Ihh plays a key role in co-coordinating proliferation and differentiation of chondrocytes and in osteoblast development in the long bones; as a result long bones of *Ihh* mutants are one-fifth of their normal length at birth and have no bone (Karp et al., 2000; Long et al., 2001; Pathi et al., 1999; St-Jacques et al., 1999; Vortkamp et al., 1996). Surprisingly, long bone

development in *Disp1*$^{\Delta 2/C829F}$, *Ihh*+/– was normal at birth. This result suggests two possibilities. First, Ihh signaling in the bone is independent of Disp1 activity. The second possibility is that Ihh signaling is Disp1-dependent in the bone, but relatively low levels of signaling suffice, as in the induction of the dorsalmost ventral progenitor populations in the neural tube and sclerotome of the somites, where Shh is the key signaling factor. Distinguishing between these possibilities will require a specific removal of *Disp1* activity from the developing skeleton.

In summary, our genetic interaction studies connect Disp1 specifically to the Hh pathway. Furthermore, our studies reveal a spectrum of responses to the attenuation of Hh-signaling strength in various Hh-dependent target fields, which might relate to tissue-specific (epithelial versus mesenchymal) differences, or differing requirements for active ligand by responding cells.

We thank Drs Kathryn Anderson and Tamara Caspary for allowing us to use *Disp1*$^{C829F/+}$ before the publication of this allele and for helpful discussion, Jill McMahon for ES cell injection, and Diane Faria for histology. We also thank Juhee Jeong, Jeff Barrow, Tom Carroll, Jing Yu and Mark Wijgerde for critical input. For the gift of antibodies we thank Jen Jensen (Nkx6.1), Ariel Ruiz I Altaba (Hnf3β), Hirohide Takebayashi (Olig2) and Tom Jessell (Nkx2.2, Chox10). We are grateful to Dr Ma and the Beachy Laboratory for helpful discussion and the sharing of reagents (Shh::Renilla luciferase fusion construct and mDispA expression construct). This work was supported by a grant from the National Institute of Health (NS 33642).

References

Belloni, E., Muenke, M., Roessler, E., Traverso, G., Siegel-Bartelt, J., Frumkin, A., Mitchell, H. F., Donis-Keller, H., Helms, C., Hing, A. V. et al. (1996). Identification of Sonic hedgehog as a candidate gene responsible for holoprosencephaly. *Nat. Genet.* **14**, 353-356.

Briscoe, J. and Ericson, J. (2001). Specification of neuronal fates in the ventral neural tube. *Curr. Opin. Neurobiol.* **11**, 43-49.

Briscoe, J., Pierani, A., Jessell, T. M. and Ericson, J. (2000). A homeodomain protein code specifies progenitor cell identity and neuronal fate in the ventral neural tube. *Cell* **101**, 435-445.

Briscoe, J., Sussel, L., Serup, P., Hartigan-O'Connor, D., Jessell, T. M., Rubenstein, J. L. and Ericson, J. (1999). Homeobox gene Nkx2.2 and specification of neuronal identity by graded Sonic hedgehog signalling. *Nature* **398**, 622-627.

Bumcrot, D. A., Takada, R. and McMahon, A. P. (1995). Proteolytic processing yields two secreted forms of sonic hedgehog. *Mol. Cell. Biol.* **15**, 2294-2303.

Burke, R., Nellen, D., Bellotto, M., Hafen, E., Senti, K. A., Dickson, B. J. and Basler, K. (1999). Dispatched, a novel sterol-sensing domain protein dedicated to the release of cholesterol-modified hedgehog from signaling cells. *Cell* **99**, 803-815.

Cai, J., Xu, X., Yin, H., Wu, R., Modderman, G., Chen, Y., Jensen, J., Hui, C. C. and Qiu, M. (2000). Evidence for the differential regulation of Nkx-6.1 expression in the ventral spinal cord and foregut by Shh-dependent and -independent mechanisms. *Genesis* **27**, 6-11.

Caspary, T., Garcia-Garcia, M. J., Huangfu, D., Eggenschwiler, J. T., Wyler, M. R., Rakeman, A. S., Alcorn, H. L. and Anderson, K. V. (2002). Mouse dispatched homolog1 is required for long-range, but not juxtacrine, Hh signaling. *Curr. Biol.* **12**, 1628-1632.

Chamoun, Z., Mann, R. K., Nellen, D., von Kessler, D. P., Bellotto, M., Beachy, P. A. and Basler, K. (2001). Skinny hedgehog, an acyltransferase required for palmitoylation and activity of the hedgehog signal. *Science* **293**, 2080-2084.

Chen, Y. and Struhl, G. (1996). Dual roles for patched in sequestering and transducing Hedgehog. *Cell* **87**, 553-563.

Chiang, C., Litingtung, Y., Lee, E., Young, K. E., Corden, J. L., Westphal, H. and Beachy, P. A. (1996). Cyclopia and defective axial patterning in mice lacking Sonic hedgehog gene function. *Nature* **383**, 407-413.

Chuang, P. T. and McMahon, A. P. (1999). Vertebrate Hedgehog signalling modulated by induction of a Hedgehog- binding protein. *Nature* **397**, 617-621.

Denef, N., Neubuser, D., Perez, L. and Cohen, S. M. (2000). Hedgehog induces opposite changes in turnover and subcellular localization of patched and smoothened. *Cell* **102**, 521-531.

Ding, Q., Motoyama, J., Gasca, S., Mo, R., Sasaki, H., Rossant, J. and Hui, C. C. (1998). Diminished Sonic hedgehog signaling and lack of floor plate differentiation in Gli2 mutant mice. *Development* **125**, 2533-2543.

Ericson, J., Briscoe, J., Rashbass, P., van Heyningen, V. and Jessell, T. M. (1997a). Graded sonic hedgehog signaling and the specification of cell fate in the ventral neural tube. *Cold Spring Harbor Symp. Quant. Biol.* **62**, 451-466.

Ericson, J., Morton, S., Kawakami, A., Roelink, H. and Jessell, T. M. (1996). Two critical periods of Sonic Hedgehog signaling required for the specification of motor neuron identity. *Cell* **87**, 661-673.

Ericson, J., Rashbass, P., Schedl, A., Brenner-Morton, S., Kawakami, A., van Heyningen, V., Jessell, T. M. and Briscoe, J. (1997b). Pax6 controls progenitor cell identity and neuronal fate in response to graded Shh signaling. *Cell* **90**, 169-180.

Fan, C. M., Porter, J. A., Chiang, C., Chang, D. T., Beachy, P. A. and Tessier-Lavigne, M. (1995). Long-range sclerotome induction by sonic hedgehog: direct role of the amino-terminal cleavage product and modulation by the cyclic AMP signaling pathway. *Cell* **81**, 457-465.

Gallet, A., Rodriguez, R., Ruel, L. and Therond, P. (2003). Cholesterol modification of hedgehog is required for trafficking and movement, revealing an asymmetric cellular response to hedgehog. *Dev. Cell* **4**, 191-204.

Gao, B., Guo, J., She, C., Shu, A., Yang, M., Tan, Z., Yang, X., Guo, S., Feng, G. and He, L. (2001). Mutations in IHH, encoding Indian hedgehog, cause brachydactyly type A-1. *Nat. Genet.* **28**, 386-388.

Goodrich, L. V., Johnson, R. L., Milenkovic, L., McMahon, J. A. and Scott, M. P. (1996). Conservation of the hedgehog/patched signaling pathway from flies to mice: induction of a mouse patched gene by Hedgehog. *Genes Dev.* **10**, 301-312.

Hammerschmidt, M., Bitgood, M. J. and McMahon, A. P. (1996). Protein kinase A is a common negative regulator of Hedgehog signaling in the vertebrate embryo. *Genes Dev.* **10**, 647-658.

Hatini, V., Huh, S. O., Herzlinger, D., Soares, V. C. and Lai, E. (1996). Essential role of stromal mesenchyme in kidney morphogenesis revealed by targeted disruption of Winged Helix transcription factor BF-2. *Genes Dev.* **10**, 1467-1478.

Hu, D. and Helms, J. A. (1999). The role of sonic hedgehog in normal and abnormal craniofacial morphogenesis. *Development* **126**, 4873-4884.

Ingham, P. W. and McMahon, A. P. (2001). Hedgehog signaling in animal development: paradigms and principles. *Genes Dev.* **15**, 3059-3087.

Jessell, T. M. (2000). Neuronal specification in the spinal cord: inductive signals and transcriptional codes. *Nat. Rev. Genet.* **1**, 20-29.

Johnson, R. L., Rothman, A. L., Xie, J., Goodrich, L. V., Bare, J. W., Bonifas, J. M., Quinn, A. G., Myers, R. M., Cox, D. R., Epstein, E. H., Jr et al. (1996). Human homolog of patched, a candidate gene for the basal cell nevus syndrome. *Science* **272**, 1668-1671.

Karp, S. J., Schipani, E., St-Jacques, B., Hunzelman, J., Kronenberg, H. and McMahon, A. P. (2000). Indian hedgehog coordinates endochondral bone growth and morphogenesis via parathyroid hormone related-protein-dependent and -independent pathways. *Development* **127**, 543-548.

Kawakami, T., Kawcak, T., Li, Y.-J., Zhang, W., Hu, Y. and Chuang, P. T. (2002). Mouse Dispatched mutants fail to distribute hedgehog proteins and are defective in hedgehog signaling. *Development* **129**, 5753-5765.

Kume, T., Deng, K. and Hogan, B. (2000). Minimal Phenotype of Mice Homozygous for a Null Mutation in the Forkhead/Winged Helix Gene, *Mf2*. *Mol. Cell. Biol.* **20**, 1419-1425.

Lewis, P. M., Dunn, M. P., McMahon, J. A., Logan, M., Martin, J. F., St-Jacques, B. and McMahon, A. P. (2001). Cholesterol modification of sonic hedgehog is required for long-range signaling activity and effective modulation of signaling by Ptc1. *Cell* **105**, 599-612.

Long, F., Zhang, X. M., Karp, S., Yang, Y. and McMahon, A. P. (2001). Genetic manipulation of hedgehog signaling in the endochondral skeleton reveals a direct role in the regulation of chondrocyte proliferation. *Development* **128**, 5099-5108.

Ma, Y., Erkner, A., Gong, R., Yao, S., Taipale, J., Basler, K. and Beachy, P. A. (2002). Hedgehog-Mediated patterning of the mammalian embryo requires transporter-like function of Dispatched. *Cell* **111**, 63-75.

Marti, E., Bumcrot, D. A., Takada, R. and McMahon, A. P. (1995).

Requirement of 19K form of Sonic hedgehog for induction of distinct ventral cell types in CNS explants. *Nature* **375**, 322-325.

Masuya, H., Sagai, T., Wakana, S., Moriwaki, K. and Shiroishi, T. (1995). A duplicated zone of polarizing activity in polydactylous mouse mutants. *Genes Dev*. **9**, 1645-1653.

Matise, M. P., Epstein, D. J., Park, H. L., Platt, K. A. and Joyner, A. L. (1998). Gli2 is required for induction of floor plate and adjacent cells, but not most ventral neurons in the mouse central nervous system. *Development* **125**, 2759-2770.

McGarvey, T. W., Maruta, Y., Tomaszewski, J. E., Linnenbach, A. J. and Malkowicz, S. B. (1998). PTCH gene mutations in invasive transitional cell carcinoma of the bladder. *Oncogene* **17**, 1167-1172.

McMahon, A. P., Ingham, P. W. and Tabin, C. J. (2003). Developmental roles and clinical significance of hedgehog signaling. *Curr. Top. Dev. Biol*. **53**, 1-114.

Meyers, E. N. and Martin, G. R. (1999). Differences in left-right axis pathways in mouse and chick: functions of FGF8 and SHH. *Science* **285**, 403-406.

Muenke, M. and Beachy, P. A. (2000). Genetics of ventral forebrain development and holoprosencephaly. *Curr. Opin. Genet. Dev*. **10**, 262-269.

Muhr, J., Jessell, T. M. and Edlund, T. (1997). Assignment of early caudal identity to neural plate cells by a signal from caudal paraxial mesoderm. *Neuron* **19**, 487-502.

Nanni, L., Ming, J. E., Bocian, M., Steinhaus, K., Bianchi, D. W., Die-Smulders, C., Giannotti, A., Imaizumi, K., Jones, K. L., Campo, M. D. et al. (1999). The mutational spectrum of the sonic hedgehog gene in holoprosencephaly: SHH mutations cause a significant proportion of autosomal dominant holoprosencephaly. *Hum. Mol. Genet*. **8**, 2479-2488.

Pabst, O., Herbrand, H., Takuma, N. and Arnold, H. H. (2000). NKX2 gene expression in neuroectoderm but not in mesendodermally derived structures depends on sonic hedgehog in mouse embryos. *Dev. Genes Evol*. **210**, 47-50.

Pathi, S., Rutenberg, J. B., Johnson, R. L. and Vortkamp, A. (1999). Interaction of Ihh and BMP/Noggin signaling during cartilage differentiation. *Dev. Biol*. **209**, 239-253.

Pepinsky, R. B., Zeng, C., Wen, D., Rayhorn, P., Baker, D. P., Williams, K. P., Bixler, S. A., Ambrose, C. M., Garber, E. A., Miatkowski, K. et al. (1998). Identification of a palmitic acid-modified form of human Sonic hedgehog. *J. Biol. Chem*. **273**, 14037-14045.

Placzek, M., Tessier-Lavigne, M., Yamada, T., Jessell, T. M. and Dodd, J. (1990). Mesodermal control of neural cell identity: floor plate induction by the notochord. *Science* **250**, 985-988.

Porter, J. A., Ekker, S. C., Park, W. J., von Kessler, D. P., Young, K. E., Chen, C. H., Ma, Y., Woods, A. S., Cotter, R. J., Koonin, E. V. et al. (1996). Hedgehog patterning activity: role of a lipophilic modification mediated by the carboxy-terminal autoprocessing domain. *Cell* **86**, 21-34.

Rallu, M., Machold, R. P., Gaiano, N., Corbin, J. G., McMahon, A. P. and Fishell, G. (2002). Dorsoventral patterning is established in the telencephalon of mutants lacking both Gli3 and Hedgehog signaling. *Development* **129**, 4963-4974.

Roelink, H., Porter, J. A., Chiang, C., Tanabe, Y., Chang, D. T., Beachy, P. A. and Jessell, T. M. (1995). Floor plate and motor neuron induction by different concentrations of the amino-terminal cleavage product of sonic hedgehog autoproteolysis. *Cell* **81**, 445-455.

Ruiz i Altaba, A., Jessell, T. M. and Roelink, H. (1995). Restrictions to floor plate induction by hedgehog and winged-helix genes in the neural tube of frog embryos. *Mol. Cell. Neurosci*. **6**, 106-121.

Schaeren-Wiemers, N. and Gerfin-Moser, A. (1993). A single protocol to detect transcripts of various types and expression levels in neural tissue and cultured cells: in situ hybridization using digoxigenin-labelled cRNA probes. *Histochemistry* **100**, 431-440.

St-Jacques, B., Dassule, H. R., Karavanova, I., Botchkarev, V. A., Li, J., Danielian, P. S., McMahon, J. A., Lewis, P. M., Paus, R. and McMahon, A. P. (1998). Sonic hedgehog signaling is essential for hair development. *Curr. Biol*. **8**, 1058-1068.

St-Jacques, B., Hammerschmidt, M. and McMahon, A. P. (1999). Indian hedgehog signaling regulates proliferation and differentiation of chondrocytes and is essential for bone formation. *Genes Dev*. **13**, 2072-2086.

Takebayashi, H., Yoshida, S., Sugimori, M., Kosako, H., Kominami, R., Nakafuku, M. and Nabeshima, Y. (2000). Dynamic expression of basic helix-loop-helix Olig family members: implication of Olig2 in neuron and oligodendrocyte differentiation and identification of a new member, Olig3. *Mech. Dev*. **99**, 143-148.

Taylor, F. R., Wen, D., Garber, E. A., Carmillo, A. N., Baker, D. P., Arduini, R. M., Williams, K. P., Weinreb, P. H., Rayhorn, P., Hronowski, X. et al. (2001). Enhanced potency of human Sonic hedgehog by hydrophobic modification. *Biochemistry* **40**, 4359-4371.

Vortkamp, A., Lee, K., Lanske, B., Segre, G. V., Kronenberg, H. M. and Tabin, C. J. (1996). Regulation of rate of cartilage differentiation by Indian hedgehog and PTH-related protein. *Science* **273**, 613-622.

Wallis, D. E. and Muenke, M. (1999). Molecular mechanisms of holoprosencephaly. *Mol. Genet. Metab*. **68**, 126-138.

Wijgerde, M., McMahon, J., Rule, M. and McMahon, A. (2002). A direct requirement for Hedgehog signaling for normal specification of all ventral progenitor domains in the presumptive mammalian spinal cord. *Genes Dev*. **16**, 2849-2864.

Wilkinson, D. G. (1992). Whole mount in situ hybridization to vertebrate embryos. In *In Situ Hybridization: A Pratical Approach*, pp. 75-83. Oxford, UK: IRL Press.

Yamada, T., Placzek, M., Tanaka, H., Dodd, J. and Jessell, T. M. (1991). Control of cell pattern in the developing nervous system: polarizing activity of the floor plate and notochord. *Cell* **64**, 635-647.

Zeng, X., Goetz, J. A., Suber, L. M., Scott, W. J., Schreiner, C. M. and Robbins, D. J. (2001). A freely diffusible form of Sonic hedgehog mediates long-range signaling. *Nature* **411**, 716-719.

Zhang, M., Dwyer, N. K., Love, D. C., Cooney, A., Comly, M., Neufeld, E., Pentchev, P. G., Blanchette-Mackie, E. J. and Hanover, J. A. (2001a). Cessation of rapid late endosomal tubulovesicular trafficking in Niemann-Pick type C1 disease. *Proc. Natl. Acad. Sci. USA* **98**, 4466-4471.

Zhang, X. M., Ramalho-Santos, M. and McMahon, A. P. (2001b). Smoothened mutants reveal redundant roles for Shh and Ihh signaling including regulation of L/R symmetry by the mouse node. *Cell* **106**, 781-792.